HHS Public Access

Author manuscript

J Neurochem. Author manuscript; available in PMC 2019 October 01.

Published in final edited form as:

J Neurochem. 2018 October ; 147(2): 222–239. doi:10.1111/jnc.14555.

The mGluR5 positive allosteric modulator VU0409551 improves synaptic plasticity and memory of a mouse model of Huntington's disease

Juliana G. Doria[#*], **Jessica M. de Souza**[#*], **Flavia R. Silva**[*], **Isabella G. Olmo**[*], **Toniana G. Carvalho**[*], **Juliana Alves-Silva**[*], **Talita H. Ferreira-Vieira**[*], **Jessica T. Santos**[*], **Claudymara Q. S. Xavier**[*], **Nathalia C. Silva**[*], **Esther M. A. Maciel**[*], **Peter Jeffrey Conn**[†], and **Fabiola M. Ribeiro**[*]

[*]Department of Biochemistry and Immunology, Institute of Biological Sciences (ICB), Universidade Federal de Minas Gerais, Belo Horizonte, MG, Brazil

[†]Vanderbilt Center for Drug Discovery, Vanderbilt University, Nashville, TN, USA

[#] These authors contributed equally to this work.

Abstract

Huntington's Disease (HD) is an autosomal-dominant neurodegenerative disorder, characterized by involuntary body movements, cognitive impairment, and psychiatric disorder. The metabotropic glutamate receptor 5 (mGluR5) plays an important role in HD and we have recently demonstrated that mGluR5-positive allosteric modulators (PAMs) can ameliorate pathology and the phenotypic signs of a mouse model of HD. In this study, we investigated the molecular mechanisms involved in mGluR5 PAMs effect on memory. Our results demonstrate that subchronic treatment with the mGluR5 PAM VU0409551 was effective in reversing the memory deficits exhibited by BACHD mice, a mouse model for HD. Moreover, VU0409551 treatment stabilized mGluR5 at the cellular plasma membrane of BACHD mice, increasing the expression of several genes important for synaptic plasticity, including c-Fos, brain-derived neurotrophic factor, Arc/Arg3.1, syntaxin 1A, and post-synaptic density-95. In addition, VU0409551 treatment also increased dendritic spine density and maturation and augmented the number of pre-synaptic sites. In conclusion, our results demonstrate that VU0409551 triggered the activation of cell signaling pathways important for synaptic plasticity, enhancing the level of dendritic spine maturation and rescuing BACHD memory impairment.

Address correspondence and reprint requests to Dr Fabiola M. Ribeiro, Department of Biochemistry and Immunology, Institute of Biological Sciences (ICB), Universidade Federal de Minas Gerais, Ave. Antonio Carlos 6627, Belo Horizonte, MG, CEP: 31270-901, Brazil. fmribeiro@icb.ufmg.br.

Open Science Badges

This article has received a badge for *__Open Materials__* because it provided all relevant information to reproduce the study in the manuscript. The complete Open Science Disclosure form for this article can be found at the end of the article. More information about the Open Practices badges can be found at https://cos.io/our-services/open-science-badges/.

Supporting information

Additional supporting information may be found online in the Supporting Information section at the end of the article.

Keywords

Huntington's disease; memory; metabotropic glutamate receptor 5; synaptic plasticity; VU0409551

Huntington's disease (HD) is a hereditary and progressive neurodegenerative disorder caused by an expansion of the glutamine-encoding CAG tract present in the first exon of the huntingtin (HTT) gene (Group 1993). Despite its ubiquitous expression, mutant HTT protein triggers selective neuronal cell loss in the striatum and cortex and, as disease progresses, it also affects the hippocampus and hypothalamus (Vonsattel *et al.* 1985; Vonsattel 2008). HD symptoms include movement disorder, psychological disturbance, and cognitive dysfunction (Li and Li 2004; Vonsattel 2008). Notably, cognitive deficits can be detected in pre-motormanifest HD patients, gradually worsening in later stages of the disease (Baake *et al.* 2017).

The metabotropic glutamate receptor 5 (mGluR5) plays a significant role in HD. mGluR5, which is highly expressed in the brain regions that are mainly affected in HD, has been shown to physically interact with both wild-type and mutant HTT (Anborgh *et al.* 2005). Moreover, mGluR5 is important for various forms of synaptic plasticity, as mGluR5 receptor antagonism and genetic ablation have been shown to impair learning and memory (Simonyi *et al.* 2010). Thus, mGluR5 is a potential pharmacological target to treat HD-related memory deficits. For instance, it has been shown that mGluR5-positive allosteric modulators (PAMs) enhance memory, facilitate hippocampal long-term potentiation (LTP) and long-term depression, and improve spatial learning (Ayala *et al.* 2009). In addition, mGluR5 PAMs rescue pharmacologically induced deficits in object recognition memory (Uslaner *et al.* 2009; Reichel *et al.* 2011). Regarding HD, we previously demonstrated that chronic treatment for 18 weeks of a transgenic mouse model of HD, the BACHD mice, with the mGluR5 PAM 3-Cyano-N-(1,3-diphenyl-1H-pyrazol-5-yl)benzamide (CDPPB) prevents neuronal cell loss, decreases HTT aggregate formation and rescues memory deficits (Doria *et al.* 2015). Moreover, we have also demonstrated that mGluR5 stimulation by CDPPB can activate cell signaling pathways that are important for neuronal survival and synaptic plasticity, including extracellular signal-regulated kinase (ERK) and brain-derived neurotrophic factor (BDNF) (Doria *et al.* 2015, 2013; Batista *et al.* 2016). Interestingly, although BACHD mice only exhibit overt neuronal cell death at 12 months of age, memory deficits can be observed as early as 6 months of age (Gray *et al.* 2008; Doria *et al.* 2015), indicating that earlier alterations other than neuronal cell death might play a role in HD-related memory disturbance. Thus, it is possible that mGluR5 PAMs improve memory impairment by enhancing synaptic plasticity in a mechanism that is independent of their neuroprotective effect. It has been demonstrated that the recently developed mGluR5 PAM, [6,7-Dihydro-2-(phenox-ymethyl)oxazolo[5,4-*c*]pyridin-5(4*H*)-yl](fluorophenyl) methanone (VU0409551), exhibits superior pharmacokinetics, as compared to other mGluR5 PAMs, such as CDPPB, and facilitates synaptic plasticity by potentiating an N-methyl-D-aspartate receptor (NMDAR)-independent form of long-term depression (Rook *et al.* 2015). Therefore, in this study, we decided to determine whether VU0409551 could rescue BACHD memory deficits.

Subchronic administration of 3 mg/Kg VU0409551 intraperitoneal (i.p.) for 8 days fully rescued the cognitive impairment exhibited by 8- to 10-month-old BACHD mice. Interestingly, VU0409551 treatment increased mGluR5 plasma membrane expression in BACHD mice, potentiating its intracellular signaling pathways. As a consequence, there was an up-regulation of the expression levels of genes that are important for synaptic plasticity, including BDNF, cytoskeletal-associated protein (Arc/Arg3.1), c-Fos, syntaxin 1A, and post-synaptic density-95 (PSD-95), as well as an increase in the density of mature spines and pre-synaptic terminals in mice treated with VU0409551. Thus, our results shed light on the mechanisms involved in VU0409551-induced memory enhancement and suggest that mGluR5 PAMs may have promise as therapeutic agents used to prevent the cognitive deficits typical of HD.

Material and methods

Material

Neurobasal medium (CAT #21103049), N2 (CAT #17502-048) and B27 (CAT #0080085SA) supplements, GlutaMAX (50 mg/mL penicillin and 50 mg/mL streptomycin) (CAT #35050-061), Live/Dead viability assay (CAT #L3224), TRIzol (CAT #15596-018), Nuclease-Free Water (CAT #750023), Power SYBR® Green PCR Master Mix (CAT # #4367659), and NeutrAvidin bead (CAT # #29200) were purchased from Thermo Fisher Scientific, Waltham, MA, USA. Vectastain Elite ABC Kit (Mouse IgG) (CAT #PK-6102) and Vector SG Peroxidase Substrate Kit (CAT #PK-6101) where purchased from Vector laboratories, Burlingame, CA, USA. Entellan® (CAT #107960) was from Merck, Kenilworth, NJ, USA. Horseradish peroxidase-conjugated anti-rabbit IgG secondary antibody (CAT #170-6515) was from Bio-Rad Laboratories, Hercules, CA, USA. FD Rapid GolgiStain™ (CAT #PK401) was purchased from FD NeuroTechnologies, Columbia, MD, USA. Rabbit anti-c-Fos polyclonal antibody (CAT #sc-52, RRID:AB_2629503) was obtained from Santa Cruz Biotechnology, Minneapolis, MN, USA. Rabbit anti-mGluR5 polyclonal antibody (CAT #AB5675, RRID: AB_2295173) was obtained from Millipore, Burlington, MA, USA. Mouse monoclonal anti-synaptotagmin 2 (CAT #znp-1, RRID: AB_10013783) was from DSHB, Iowa City, IA, USA. ECL Western blotting detection reagents (CAT # #RPN2232) were purchased from GE Healthcare, Chicago, IL, USA. VU0409551 was kindly donated by Dr P. J. Conn. Rabbit anti-β-actin polyclonal antibody (CAT #A2228) and other biochemical reagents were purchased from Sigma–Aldrich, Saint Louis, MO, USA. This study was not pre-registered.

Mouse model

FVB/NJ (wild type, RRID:IMSR_JAX:001800) and FVB/N -Tg(HTT*97Q)IXwy/J (BACHD) transgenic mice (Gray *et al.* 2008) were purchased from Jackson Laboratory (RRID: IMSR_JAX:008197, http://jaxmice.jax.org/strain/008197.html) (Bar Harbor, ME, USA). C57BL/6 mice (25–30 g) were purchased from the animal facility from the Universidade Federal de Minas Gerais. Mice were housed in an animal care facility at 23°C on a 12 h light/12 h dark cycle with food and water provided *ad libitum.* Animal care was in accordance with the Universidade Federal de Minas Gerais – Ethics Committee on Animal Experimentation, CEUA 35/2015. A total of 33 wild-type (WT) and 31 BACHD male mice

and 6 female C57BL/6 mice were used for this study. All mice that were killed in this study were first anesthetized with ketamine/xylazine (80/8 mg/kg) i.p. before cervical dislocation. Predicted sample size was calculated using the formula $IC=2\times SD/n^{-2}$ (IC, confidence interval; SD, standard deviation; *n*, sample size).

Neuronal primary culture preparation

Neuronal cultures were prepared from either the striatal region of E15 mouse embryo brains or the hippocampus of E19 mouse embryo brains. After dissection, striatal or hippocampal tissue was submitted to trypsin digestion followed by cell dissociation using a fire-polished Pasteur pipette. Cells were plated on poly-L-ornithine-coated dishes in Neurobasal medium supplemented with N2 and B27 supplements, 2 mM GlutaMAX, 50 μg/mL penicillin, and 50 μg/mL streptomycin. Cells were incubated at 37°C and 5% CO_2 in a humidified incubator and cultured for 10–12 days *in vitro* with medium replenishment every 4 days.

Cell death assay

Neurons were incubated for 20 h with either vehicle (Hank's balanced salt solution) or 50 μM glutamate, in the presence or absence of V0409551, as indicated in the *Figure Legend,* and cell death was determined by Live/Dead viability assay, as described previously (Doria *et al.* 2013). Briefly, neurons were stained with 2 μM calcein acetoxymethyl ester (AM) and 2 μM ethidium homodimer-1 for 15 min and the fractions of live (calcein AM positive) and dead (ethidium homodimer-1 positive) cells were determined. Neurons were visualized by fluorescence microscopy EVOS® FLoid® Cell Imaging Station (Thermo Scientific, Waltham, MA, USA) and scored by a blinded observer. A minimum of 300 cells were analyzed per well in triplicate using ImageJ™ software. Dead cells were expressed as a percentage of the total number of cells.

Drug administration

VU0409551 was dissolved in 20% β-cyclodextrin and injected intraperitoneal (i.p.) at a volume of 4 mL/Kg. Male WT and BACHD mice were allocated in two groups, Vehicle and Drug, by simple randomization. Either vehicle (20% β-cyclodextrin) or VU0409551 3 mg/Kg were delivered to 8- to 10-month-old WT and BACHD mice once a day during a total of 8 days. The behavioral tests were performed on day 7 and 8. On day 8, mice were anesthetized with ketamine (80 mg/kg) and xylazine (10 mg/kg) intraperitoneally (i.p.) and killed, and brain tissue was utilized for protein and gene expression analyses.

Open field

To measure spontaneous locomotor activity, male WT and BACHD mice treated with either vehicle or 3 mg/Kg VU0409551 for 7 days were subjected to the open field apparatus (LE 8811 IR Motor Activity Monitors PANLAB, Harvard Apparatus), which consists of a 450 × 450 × 200 mm acrylic box. Animals were placed in the open field apparatus and the horizontal activity (distance travelled) and center distance was assessed during 60 min. All sessions were performed during the first part of the light cycle and mice were acclimated to the room for at least 30 min before the beginning of each session. Quantification of the total activity was calculated using the ACTITRACK program.

Object recognition

Male WT and BACHD mice treated with either vehicle or 3 mg/Kg VU0409551 were submitted to object recognition test. This memory test is based on mice preferential spontaneous exploration of objects placed at a novel location. The apparatus used was an open box made of polyvinyl chloride (PVC) 50 cm × 35 cm × 25 cm surmounted by a video camera and a light. Two identical objects made of glass or plastic were used. Objects weight was such that they could not be displaced by mice. As far as we could ascertain, they had no natural significance for mice and they had never been associated with reinforcement. Initial tests showed that mice did not have any preference for the objects used. The general procedure consisted of three different phases: a familiarization phase, a training phase, and a test phase. On the first day (VU0409551 treatment day 7), mice were individually submitted to a single familiarization session of 10 min, during which they were introduced to the empty arena. Twenty hours later (VU0409551 treatment day 8), animals were submitted to a single 10-min training session during which two identical objects were placed in symmetrical positions from the center of the arena and each object was 15 cm from the side walls. After a 90-min delay, during which mice returned to their home cage, animals were reintroduced into the arena for 10 min (test phase) and exposed to the same objects, but one of the objects was displaced to a novel position. To control odor cues, the apparatus was cleaned with 70% ethanol and ventilated between each session and animal. All sessions were performed during the first part of the light cycle and mice were acclimated to the room for at least 15 min before the beginning of each session. Exploration time was defined as sniffing or touching the object with the nose. Data are expressed as recognition index, calculated according to the following formulae: (i) Training phase: time exploring object 1 × 100/(time exploring object 1 + time exploring object 2); (ii) Test phase: time exploring the object 1 placed at the new location × 100/(time exploring the object 2 placed at the familiar + time exploring the object 1 placed at the new location) (Lazaroni *et al.* 2012).

Cued fear conditioning test

Male WT and BACHD mice treated with either vehicle or 3 mg/Kg VU0409551 for 8 days were subjected to cued fear conditioning test. Mice were placed in a conditioning chamber 23 × 23 × 30 cm Plexiglas box with black walls (Insight Equipamentos). Floor was made of stainless-steel grid rods (0.4 cm in diameter, spaced 0.6 cm apart) and at the sealing there was a video camera system. Chamber was located inside a soundproof box. First, mice were allowed to freely explore the chamber for 120 s. To induce conditioning, a tone (CS: conditioned stimulus; 85 dB, 1KHz) was delivered for 30 s, being the last 2 s paired with foot-shock (US: unconditioned stimulus; 0.7 mA). The presentation of the CS-US paring was repeated five times to strengthen the association, with 30 s interval between each paring. After 60 s, animals were placed into their home cage. After 90 min, mice were allocated into another chamber, providing a different context for the testing phase. This novel chamber had the same size as the previous one (training phase), but black and white walls and different smell. After staying in this new chamber for 180 s, animals were exposed during additional 180 s to the same tone (CS) used for conditioning, but in the absence of foot-shock. Freezing behavior, defined as a complete lack of movement, except for respiration, was scored for 2 s every 5 s during the entire period animals remained in the novel chamber (Radwanska *et al.* 2011).

Cell surface biotinylation assay

The biotinylation assay was performed as described previously (Silva *et al.* 2017). The striatum and hippocampus of WT and BACHD mice treated with either vehicle or 3 mg/Kg VU0409551 for 8 days were dissected and sliced (300 μm) using a McIlwain tissue chopper. Slices were recovered in artificial cerebrospinal fluid (ACSF) (127 mM NaCl, 2 mM KCl, 10 mM glucose, 1.2 mM KH2PO4, 26 mM NaH_2CO_3, 1 mM $MgSO_4$, 1 mM $CaCl_2$, pH 7.4) gassed with 95% O_2/5% CO_2 and incubated in a shaking bath at 37°C for 30 min. Plasma membrane proteins of hippocampal and striatal slices were biotinylated with 1 mg/mL sulfo-NHS-SS-biotin (Thermo Scientific) for 1 h on ice. To quench the biotinylation reaction, slices were washed and incubated for 30 min with cold 100 mM glycine in ACSF, followed by three washes with cold ACSF. Slices were then lysed in RIPA buffer (0.15 M NaCl, 0.05 M tris-HCl, pH 7.2, 0.05 M EDTA, 1% Nonidet P40, 1% Triton X-100, 0.5% sodium deoxycholate, 0.1% SDS) containing SigmaFast™ Protease Inhibitor Cocktail Tablets. Biotinylated proteins were separated from non-biotinylated proteins by NeutrAvidin bead pull-down from equivalent amounts of total cellular protein from each sample; 80 μg of total cellular proteins for each sample were saved to determine mGluR5 total cellular expression. Biotinylated proteins and total cellular proteins were subjected to SDS-PAGE, followed by electroblotting onto nitrocellulose membranes.

Immunoblotting

The striatum and hippocampus of WT and BACHD mice treated with either vehicle or 3 mg/Kg VU0409551 for 8 days were dissected and lysed in RIPA buffer containing SigmaFast™ Protease Inhibitor Cocktail Tablets. Total cellular protein (80 μg) for each sample was subjected to SDS-PAGE, followed by immunoblotting onto nitrocellulose membranes. Membranes were blocked with 5% bovine serum albumin (BSA) in wash buffer (150 mM NaCl, 10 mM Tris-HCl, pH 7.0, and 0.05% Tween 20) for 1 h and then incubated with either rabbit anti-c-Fos (sc-253) (1 : 700) or rabbit anti-mGluR5 (1 : 500) antibodies in wash buffer containing 3% BSA at 4°C overnight. Membranes were rinsed three times with wash buffer and then incubated with secondary peroxidase-conjugated anti-rabbit IgG antibody diluted 1 : 5000 in wash buffer containing 3% skim milk for 1 h. Membranes were rinsed three times with wash buffer and incubated with ECL western blotting detection reagents. Antibodies were then stripped and membranes were incubated with rabbit anti-β-actin (1 : 1000) antibody for 2 h and probed with secondary antibody anti-rabbit IgG diluted 1 : 5000. Non-saturated, immunoreactive c-Fos and mGluR5 bands were quantified by scanning densitometry. Immunoband intensity was calculated using Image J™ software to determine the number of pixels of c-Fos and mGluR5 bands.

Quantitative RT-PCR

The striatum and hippocampus of WT and BACHD mice treated with either vehicle or 3 mg/Kg VU0409551 for 8 days were dissected and used for RNA extraction. RNA was isolated using TRIzol® reagent as per manufacturer's instructions. RNA was re-suspended in 20 μL of nuclease-free water, and its concentration and quality was analyzed by NanoDropTM (Thermo Scientific) and gel electrophoresis, respectively. cDNAs were prepared from 2 μg of total RNA extracted in a 20 μL final reverse transcription reaction.

Quantitative RT-PCR (RT-qPCR) was performed using the Power SYBR® Green PCR Master Mix in the QuantStudio™ 7 Flex real-time PCR system platform (Applied Biosystems). RT-qPCR was performed to quantify mRNA levels of the brain-derived neurotrophic factor – *BDNF (NM_001285416.1),* activity regulated cytoskeleton associated protein – *Arc (NM_018790.3),* syntaxin 1A *(NM_016801.3),* and post-synaptic density protein PSD-95 – Dgl4 (NM_007864.3). Primers were designed using Primer3Plus Program (Agerman *et al.* 2003). BDNF *(forward: 5′ ATGAAAGAAGTAAACGTCCAC 3′; reverse 5′ CCAGCAGAAAGAGTAGAGGAG 3′),* ARC (forward 5′ GCTGAAGCAGCAGACCTGA 3′; reserve 5′ TTCACTGGTATGAATCACTGCTG 3′), syntaxin 1A (forward: 5′ GAACAAAGTTCGCTCCAAGC 3′; reverse: 5′ GTGGCGTTGTACTCGGACAT 3′) and PSD-95 (forward: 5′ TCTGTGCGAGAGGTAGCAGA 3′; reverse 5′ AAGCACTCCGTGAACTCCTG 3′). The BDNF set of primers allows the detection of all the 12 BDNF transcript variants. Previous verification of undesired secondary formations or dimers between primers were performed using 'OligoAnalyser 3.1' tool (Integrated DNA Tecnology©), available at https://www.idtdna.com/calc/an alyzer. All primers used in this work were validated by serial dilution assay and the reaction efficiency was calculated, comprising 90–110% (data not shown). Samples were prepared in triplicate and changes in gene expression were determined with the $2^{-\Delta Ct}$ method using actin for normalization.

Golgi-Cox staining

WT and BACHD mice treated with either vehicle or 3 mg/Kg VU0409551 for 8 days were killed and brains were removed and stained with the FD Rapid GolgiStain™ kit (FD NeuroTechnologies), following manufacturer's instructions. Briefly, brains were immersed in an impregnation solution (A + B), which was replaced after 6 h, and then kept in dark for 14 days. Afterward, brains were transferred into solution C, which was replaced after 24 h, and kept in dark for 72 h. Brains were coronally sectioned generating 100 μm slices using a cryostat. Slices were then mounted on gelatin-coated microscope slides, stained, dehydrated, and cover-slipped with Entellan®.

Image acquisition and dendritic spine analyses

Pyramidal hippocampal neurons were chosen for analyses according to the following criteria: (i) Cell completely filled with Golgi-Cox stain; (ii) No overlap with other cell to ensure no bias of confusion; (iii) Cell body well defined; (iv) Intact primary dendrite ramification; (v) Presence of secondary or tertiary ramification measuring at least 20 μm. A total of 12–15 Z-stack images per animal were acquired using a confocal microscope (Nikon Eclipse C2 with a ×63 objective-oil) by a blinded observer. Measurement and classification of the dendritic spines were performed using the free software Image J™ and RECONSTRUCT, available at (http://synapses.clm.utexas.edu), as previously described (Risher *et al.* 2014).

Immunofluorescence and imaging

WT and BACHD mice treated with either vehicle or 3 mg/Kg VU0409551 for 8 days were anesthetized with ketamine/xylazine (80/8 mg/kg) i.p. and transcardially perfused with phosphate-buffered saline (PBS). Brains were dissected and stored in 4% paraformaldehyde

in PBS for 72 h and then infiltrated with 30% sucrose in PBS. Brains were coronally sectioned using a cryostat and 30 μm slices were stored in cryoprotect solution. Sections were washed three times for 30 min with tris-buffered saline (TBS) and 0.5% Triton X-100. Then, slices were incubated for 30 min in citrate buffer at 70°C, washed three times for 10 min and blocked for 120 min using 4% BSA in TBS and 0.5% Triton X-100. Sections were incubated with mouse anti-synaptotagmin 2 (1 : 500) primary antibody in blocking solution overnight at 4°C. Sections were washed three times for 10 min in TBS and 0.5% Triton X-100 and then incubated with goat anti-mouse antibody conjugated to Alexa Fluor 488 1:500 in blocking solution for 60 min at 25°C. Finally, sections were washed 6 times for 10 min with TBS and 0.5% Triton X-100. Sections were mounted on slides and fluorescence microscopy was performed using a Zeiss LSM 880 confocal system equipped with a 20x/1.30 DIC M27 objective. Image acquisition was performed by a blinded observer using the Zen 2 software. Alexa Fluor 488-labeled anti-synaptotagmin 2 antibody was detected between 499 and 552 nm and excitation of fluorophore was performed using 488 nm laser. A total of 18 images were taken from at least three animals for each condition. Fluorescence intensity of pixel gray levels was obtained blind using ImageJ software.

Data analyses

Means ± SEM are shown for the number of independent experiments indicated in *Figure Legends.* GraphPad Prism™ software was used to analyze data for statistical significance and for curve fitting. Data were tested for normality of distribution by the D'Agostino & Pearson omnibus normality test. No outliers (greater than two deviations from the mean) were found and, thus, no data were excluded. Statistical significance was determined by analysis of variance, one-way and two-way (ANOVA), followed by Bonferroni *post hoc* multiple comparison testing.

Results

VU0409551 treatment rescued BACHD mice memory deficits

BACHD mice exhibit several of the phenotypic signs typical of HD, as well as the molecular and cellular alterations that take place in the disease (Gray *et al.* 2008). The memory deficits exhibited by BACHD mice can be detected as early as at 6 months of age (Doria *et al.* 2015). Thus, in order to evaluate the effect of VU0409551 subchronic treatment on memory deficits, all behavioral tests were performed employing WT and BACHD mice at 8–10 months of age. Mice were treated with either 3 mg/kg VU0409551 or vehicle (20% β-cyclodextrin) via intraperitoneal injections daily over 8 days. The dose of 3 mg/kg was chosen based on dose–response curves performed previously (Rook *et al.* 2015). To assess the effect of VU0409551 subchronic treatment on a specific memory deficit observed in BACHD mice, we performed the novel object location recognition test, which evaluates memory based on mice preference for novelty. WT animals treated with either vehicle or VU0409551 explored the object placed at the novel location for a percentage of time significantly higher than 50% [WT-vehicle: $t_{(6)} = 3.44$; $p = 0.01$; WT-VU0409551: $t_{(7)}) = 2.97$; $p = 0.02$] (Fig. 1a), indicating that these animals exhibit intact memory. However, vehicle-treated BACHD mice failed to distinguish between the objects placed at the familiar and novel positions, confirming that this animal model exhibit memory impairment [$t_{(7)} =$

0.03; $p = 0.97$] (Fig. 1a). On the other hand, VU0409551 treatment enhanced BACHD memory, as these animals exhibited a percentage of novel location exploration very similar to that of WT controls [$t_{(8)} = 4.46$; $p = 0.002$] (Fig. 1a).

Fear is an innate defense mechanism triggered by an aversive stimulus. To determine whether VU0409551 could improve associative fear memory, we performed the cued conditioned task. In this task, the initial non-aversive neutral stimulus, which in the case of this study was sound, gains an emotional component after being paired with a noxious stimulus, such as foot-shock, generating an associative conditioned response. After learning this association, animals will respond to the previously neutral stimulus with fear behavior, such as freezing, which is characterized as total absence of movement, except for breathing (Radwanska *et al.* 2011). WT mice, treated with either vehicle or VU0409551, displayed increased freezing behavior in the presence (CS+) than in the absence (CS−) of the conditioning stimulus [WT-vehicle: $t_{(58)} = 3.45$; $p = 0.004$; WT-VU0409551: $t_{(58)} = 2.69$; $p = 0.04$] (Fig. 1b). However, freezing time of vehicle-treated BACHD mice was not different in the presence or in the absence of CS, indicating that these mice had impaired associative fear memory [$t_{(58)} = 0.95$; $p = 0.82$] (Fig. 1b). Interestingly, BACHD mice treated with VU0409551 displayed longer durations of freezing in the presence than in the absence of CS [$t_{(58)} = 3.75$; $p = 0.002$] (Fig. 1b), indicating that VU0409551 treatment can rescue BACHD associative fear memory impairment. As treatment with VU0409551 was performed for only 8 days and this length of time is not enough to prevent neuronal cell loss, these results suggest that VU0409551 ability to enhance memory is not necessarily related to its neuroprotective effect. Thus, we hypothesize that VU0409551 improves memory by facilitating synaptic plasticity.

To evaluate whether alterations in locomotion could be influencing the memory behavioral tests, spontaneous locomotor activity of WT and BACHD mice treated with either VU0409551 or vehicle were evaluated using the open field apparatus. There was no significant difference in the total distance travelled when comparing all tested groups [Genotype: $F_{(1,29)} = 0.46$, $p = 0.83$; Treatment: $F_{(1,29)} = 0.26$, $p = 0.62$; Interaction: $F_{(1,29)} = 0.66$, $P = 0.42$] (Fig. 1c and d). The percentage of time mice spend at the center of the apparatus is regarded as an indication of anxiolytic behavior, as rodents tend to spend more time closer to the walls of the apparatus than in the center of the arena, an unprotected environment (Bailey and Crawley 2009). There were no differences in the distance travelled in the center when comparing all tested groups [Genotype: $F_{(1,29)} = 0.11$, $p = 0.74$; Treatment: $F_{(1,29)} = 0.43$, $p = 0.52$; Interaction: $F_{(1,29)} = 0.30$, $p = 0.59$] (Fig. 1e and f). Taken together, these data suggest that treatment with VU0409551 did not promote changes in locomotor activity and anxiety-associated behavior.

VU0409551 treatment enhanced mGluR5 plasma membrane expression in BACHD mice

mGluR5 stimulation leads to the activation of a wide variety of cell signaling pathways important for synaptic plasticity, which can be regulated by receptor subcellular localization (Ferreira *et al.* 2009). To investigate whether VU0409551 treatment alters mGluR5 subcellular localization, hippocampal and striatal slices obtained from WT and BACHD mice treated with either vehicle or VU0409551 were subjected to biotinylation assay to

separate plasma membrane from intracellular proteins. Statistical analyses indicated that VU0409551 treatment had a significant effect on mGluR5 cell surface expression in hippocampal [Genotype: $F_{(1,12)} = 1.09$, $P = 0.32$; Treatment: $F_{(1,12)} = 6.68$, $p = 0.02$; Interaction: $F_{(1,12)} = 2.81$, $p = 0.11$] (Fig. 2a and c] and striatal slices [Genotype: $F_{(1,12)}=0.02$, $p = 0.89$; Treatment: $F_{(1,12)} = 12.80$, $p = 0.004$; Interaction: $F_{(1,12)} = 0.02$, $p = 0.89$] (Fig. 2b and d). *Post hoc* analyses indicated that VU0409551 treatment significantly increased the expression of mGluR5 at the plasma membrane of BACHD mice in both the hippocampus (Fig. 2a and c) and striatum (Fig. 2b and d). In addition, mGluR5 protein levels in total cell lysate obtained from hippocampal [Genotype: $F_{(1,20)} = 0.16$, $p = 0.69$; Treatment: $F_{(1,20)} = 0.01$, $p = 0.91$; Interaction: $F_{(1,20)} = 0.01$, $p = 0.92$] (Fig. 2e) and striatal slices [Genotype: $F_{(1,20)} = 0.65$, $p = 0.43$; Treatment: $F_{(1,20)} = 0.30$, $p = 0.59$; Interaction: $F_{(1,20)} = 0.42$, $p = 0.52$] (Fig. 2f) were not different when comparing BACHD and WT mice. Thus, unlike what would be expected for a classical agonist, VU0409551 appears to alter mGluR5 subcellular localization, favoring receptor expression at the plasma membrane.

VU0409551 increased expression of genes important for synaptic plasticity

It has been shown that VU0409551 increases ERK1/2 activation (Rook *et al.* 2015). ERK1/2 triggers the activation of transcription factors important for synaptic plasticity, including the cAMP-responsive element (CREB) (Xing *et al.* 1996). As VU0409551 treatment increased mGluR5 expression at the plasma membrane, it is possible that mGluR5-dependent cell signaling pathways might be overactivated. Therefore, we determined whether VU0409551 could increase the expression of CREB target genes that are important for synaptic plasticity. c-Fos is an immediate early gene product and its expression, which can be regulated by CREB, is widely used as a marker of neuronal activation (Fleischmann *et al.* 2003; Albasser *et al.* 2010). Since neuronal activation is an important factor contributing for synaptic plasticity, we measured c-Fos protein levels in WT and BACHD mice treated with either vehicle or VU0409551. Overall, VU0409551 treatment had a significant effect on c-Fos protein expression in the hippocampus [Genotype: $F_{(1,18)} = 1.10$, $p = 0.31$; Treatment: $F_{(1,18)} = 11.40$, $p = 0.003$; Interaction: $F_{(1,18)} = 1.34$, $p = 0.25$] (Fig. 3a and c), but not in the striatum [Genotype: $F_{(1,18)} = 0.21$, $P = 0.65$; Treatment: $F_{(1,18)} = 0.14$, $p = 0.71$; Interaction: $F_{(1,18)} = 0.51$, $p = 0.48$] (Fig. 3b and d). *Post hoc* analyses indicated that there was a significant increase in c-Fos expression levels in the hippocampus of BACHD mice treated with VU0409551 relative to that of vehicle-treated BACHD mice (Fig. 3a and c). Thus, treatment with VU0409551 promoted an increase in c-Fos levels in the hippocampus of BACHD mice, which is an indication of increased neuronal activity in this brain area.

mGluR5 activation, in addition to increase c-Fos expression levels, can also lead to increased expression levels of BDNF via ERK/CREB. BDNF plays a critical role in memory by stimulating the late phase formation of LTP and enhancing dendritic spine growth and maturation (Tyler and Pozzo-Miller 2003). Thus, we determined whether VU0409551 treatment could enhance BDNF expression. VU0409551 treatment had a significant effect on BDNF mRNA levels in the hippocampus [Genotype: $F_{(1,20)} = 3.72$, $p < 0.07$; Treatment: $F_{(1,20)} = 14.88$, $p = 0.001$; Interaction: $F_{(1,20)} = 0.23$, $p = 0.63$] (Fig. 4a), but not in the striatum [Genotype: $F_{(1,16)} = 0.43$, $p = 0.52$; Treatment: $F_{(1,16)} = 0.01$, $p = 0.91$; Interaction: $F_{(1,16)} = 0.17$, $p = 0.69$] (Fig. 4b). *Post hoc* analyses indicated that there was a significant

increase in BDNF expression in the hippocampus of BACHD mice treated with VU0409551 relative to that of vehicle-treated BACHD mice (Fig. 4a). The observed increase in BNDF mRNA levels because of VU0409551 treatment could contribute to neuroprotection. To investigate whether VU0409551 could promote neuroprotection or induce toxicity, primary cultures of striatal neurons were incubated with VU0409551 in the presence or absence of 50 μM glutamate for 20 h. Neurons treated with 50 μM glutamate exhibited higher levels of neuronal cell death, as compared to control (Figure S1A, B, C, D and G). However, when neurons were stimulated with glutamate in the presence of VU0409551 at the concentrations of 1, 10, 100, and 10 000 nM, neuronal cell death levels were substantially reduced [$F_{(4,15)}$ = 7.43, P = 0.002] (Fig. S1E, F and G). Moreover, when applied in the absence of glutamate, VU0409551 did not increase neuronal cell death above basal levels at any tested concentration [$F_{(4,16)}$ = 2.12, p = 0.13] (Fig. S1G). Similar results were observed in the case of hippocampal neurons (Fig. S2). VU0409551 treatment decreased neuronal cell death triggered by glutamate and did not increase neuronal cell death above basal levels when applied in the absence of glutamate (Fig. S2G). Thus, VU0409551 was able to protect primary cultured striatal and hippocampal neurons from glutamate insult and showed no toxic effect.

Increased expression of the activity-regulated and cytoskeletal-associated protein Arc/Arg3.1 represents a rapid response to learning experiences, stimulating mechanisms of synaptic plasticity, including the induction of LTP (Plath *et al.* 2006; Shepherd *et al.* 2006). In addition, it has been demonstrated that BDNF can increase Arc/Arg3.1 expression (Yin *et al.* 2002). Thus, we decided to determine whether VU0409551 treatment could enhance Arc/Arg3.1 expression. Mice genotype, as well as VU0409551 treatment had a significant effect on Arc/Arg3.1 expression in the hippocampus [Genotype: $F_{(1,20)}$ = 4.62, p = 0.04; Treatment: $F_{(1,20)}$ = 13.78, p = 0.001; Interaction: $F_{(1,20)}$ = 4.62, p = 0.04] (Fig. 4c), but not in the striatum [Genotype: $F_{(1,20)}$ = 0.01, p = 0.94; Treatment: $F_{(1,20)}$ = 0.01, p = 0.94; Interaction: $F_{(1,20)}$ = 0.06, p = 0.81] (Fig. 4d). *Post hoc* analyses indicated that there was a significant increase in Arc/Arg3.1 mRNA levels in the hippocampus of BACHD mice treated with VU0409551 relative to that of vehicle-treated BACHD mice (Fig. 4c). The observed increase in BDNF and Arc/Arg3.1 expression in BACHD mice may constitute an important mechanism contributing to the memory performance enhancement observed in BACHD mice treated with VU0409551.

Syntaxin 1A and PSD-95 are involved in the growth and amplification of pre- and post-synaptic terminals, respectively, enhancing synaptic transmission and contributing to synaptic plasticity (El-Husseini *et al.* 2000; Guo *et al.* 2010). Moreover, syntaxin 1A expression is also positively regulated by CREB (Guo *et al.* 2010). Thus, we decided to test whether VU0409551 treatment could also increase syntaxin 1A expression levels. Statistical analyses indicated that VU0409551 treatment had a significant effect on syntaxin 1A mRNA levels in the hippocampus [Genotype: $F_{(1,20)}$ = 0.44, p = 0.51; Treatment: $F_{(1,20)}$ = 9.32, p = 0.006; Interaction: $F_{(1,20)}$ = 2.85, p = 0.11] (Fig. 4E) and striatum [Genotype: $F_{(1,20)}$ = 0.28, p = 0.07; Treatment: $F_{(1,20)}$ = 9.09, p = 0.007; Interaction: $F_{(1,20)}$ = 1.54, p = 0.23] (Fig. 4f). *Post hoc* analyses indicated that there was a significant increase in syntaxin 1A mRNA levels in the hippocampus (Fig. 4e) and striatum (Fig. 4f) of BACHD mice treated with VU0409551 relative to that of vehicle-treated BACHD mice.

PSD-95 is regarded as a marker for the number of post-synaptic terminals (El-Husseini *et al.* 2000). Moreover, PSD-95 plays an important role in HD, as it interacts with HTT, affecting NMDAR function (Fan *et al.* 2009). As treatment with VU0409551 increased the expression of the pre-synaptic marker syntaxin 1A, we decided to determine whether PSD-95 mRNA levels were also altered following treatment. Overall, mice genotype and VU0409551 treatment had a significant effect on PSD-95 mRNA levels in the hippocampus [Genotype: $F_{(1,20)} = 5.86$, $p = 0.03$; Treatment: $F_{(1,20)} = 17.57$, $p = 0.0004$; Interaction: $F_{(1,20)} = 4.66$, $p = 0.04$] (Fig. 4g). Moreover, VU0409551 treatment also had a significant effect on PSD-95 expression levels in the striatum [Genotype: $F_{(1,20)} = 3.47$, $p = 0.08$; Treatment: $F_{(1,20)} = 5.94$, $p = 0.02$; Interaction: $F_{(1,20)} = 0.52$, $p = 0.48$] (Fig. 4f). *Post hoc* analyses indicated that there was a significant increase in PSD-95 mRNA levels in the hippocampus of BACHD mice treated with VU0409551, as compared to that of vehicle-treated WT, VU0409551-treated WT, and vehicle-treated BACHD mice (Fig. 4g). Also, PSD-95 expression levels were higher when comparing VU0409551-treated BACHD and vehicle-treated WT mice in the striatum (Fig. 4h).

VU040955 enhanced dendritic spine density and maturation and increased the number of pre-synaptic terminals

Most excitatory synapses in the mammalian brain involve dendritic spines (Hering and Sheng 2001; Nimchinsky *et al.* 2002). Dendritic spines morphology is very diverse and changes in both their density and morphology underlie modification in the strength of synaptic transmission (Hering and Sheng 2001; Nimchinsky *et al.* 2002). Our data demonstrated an increase in mGluR5 expression at the plasma membrane, as well as increased levels of PSD-95 mRNA. As PSD-95 over-expression promotes an increase in spine density (El-Husseini *et al.* 2000), we employed the Golgi-Cox impregnation technique to analyze changes in the number and morphology of dendritic spines in the hippocampus of WT and BACHD mice treated with either vehicle or VU0409551. The overall morphology and number of dendritic spines appeared to be different when comparing WT and BACHD mice treated with either vehicle or VU0409551 (Fig. 5a). Statistical analyses indicated that both mice genotype and VU0409551 treatment had a significant effect in the number of dendritic spines [Genotype: $F_{(1,47)} = 17.05$, $p = 0.0001$; Treatment: $F_{(1,47)} = 7.49$, $p = 0.009$; Interaction: $F_{(1,47)} = 0.02$, $p = 0.89$] (Fig. 5b). *Post hoc* analyses indicated that the number of dendritic spines was decreased in vehicle-treated BACHD mice, as compared to that of vehicle-treated WT mice (Fig. 5b). However, VU0409551-treated BACHD mice exhibited similar number of dendritic spines as vehicle-treated WT mice (Fig. 5b), indicating that VU0409551 treatment can normalize the number of dendritic spines in this mouse model of HD. Despite this relatively mild increase in the number of dendritic spines observed in VU0409551-treated animals, the overall volume of spines appeared greatly increased in VU0409551-treated mice (Fig. 5a), indicating that VU0409551 could be enhancing the number of larger mature spines, such as mushroom-like and branched spines. To test this hypothesis, we analyzed the morphology of each type of dendritic spines (Fig. 5c and e). Statistical analyses indicated that VU0409551 treatment had a significant effect on the number of mushroom-like spines [Genotype: $F_{(1,47)} = 0.15$, $p = 0.70$; Treatment: $F_{(1,47)} = 15.52$, $p = 0.0003$; Interaction: $F_{(1,47)} = 0.04$, $p = 0.85$]. Moreover, *post hoc* analyses indicated that VU0409551 treatment increased the number of mushroom spines in both WT

and BACHD mice, as compared to vehicle-treated controls (Fig. 5d). In the case of the branched type of spines, which is the last stage of maturation of dendritic spines, statistical analyses indicated a significant effect of both mice genotype and VU0409551 treatment on the number of branched spines [Genotype: $F_{(1,47)} = 6.16$, $p = 0.02$; Treatment: $F_{(1,47)} = 13.64$, $p = 0.0006$; Interaction: $F_{(1,47)} = 0.82$, $p = 0.37$] (Fig. 5f). *Post hoc* analyses indicated that VU0409551 treatment increased the number of branched spines in WT mice, as compared to that of vehicle-treated WT mice (Fig. 5f). Taken together, these data indicate that treatment with VU049551 increases the number of dendritic spines and accelerate spine maturation.

As we observed an increase in the number of post-synaptic sites, we decided to investigate whether VU0409551 treatment could also modify the number of pre-synaptic terminals. For that, we measured the fluorescence intensity of the pre-synaptic marker synaptotagmin 2. Synaptotagmin 2 intensity appeared increased in BACHD mice treated with VU0409551, as compared to that of vehicle-treated BACHD mice (Fig. 6a–d). Statistical analyses indicated that mice genotype had a significant effect in the levels of synaptotagmin 2 intensity [Genotype: $F_{(1,68)} = 5.49$, $p = 0.02$; Treatment: $F_{(1,68)} = 0.88$, $P = 0.35$; Interaction: $F_{(1,68)} = 9.78$, $p = 0.003$] (Fig. 6e). Moreover, *post hoc* analyses indicated that synaptotagmin 2 intensity was enhanced in VU0409551-treated BACHD mice, as compared to that of vehicle-treated BACHD and VU0409551-treated WT mice (Fig. 6e). Therefore, treatment with VU049551 increases the number of pre-synaptic terminals in BACHD mice.

Discussion

Memory impairment is a common finding in a number of neurodegenerative diseases, including Alzheimer disease, HD, and schizophrenia (Caine *et al.* 1978; Saykin *et al.* 1991; Hodges *et al.* 1992). BACHD mice recapitulate many aspects of the human neuropathology and symptoms, including formation of HTT aggregates, neuronal death, and cognitive and motor deficits (Gray *et al.* 2008). We and others have shown that the formation of HTT aggregates and neuronal death in BACHD mice only occurs at 12 months of age, although cognitive deficits are already evident at 6 months of age (Gray *et al.* 2008; Doria *et al.* 2015). At this age, BACHD mice do not exhibit overt neuronal cell loss and even if neurodegeneration was already present, VU0409551 7-day treatment would not be enough to rescue neuronal cell death. Thus, as cognitive deficits precede neuronal cell loss, we hypothesize that mGluR5 PAMs promote memory enhancement by activating synaptic plasticity mechanisms that are independent of mGluR5 PAM neuroprotective effect. We have previously demonstrated that BACHD mice exhibit a reduction in the number of synaptic vesicles in the active zone and that chronic treatment with CDPPB for 18 weeks increases the number of active zone vesicles (Doria *et al.* 2015). CDPPB effect on synaptic vesicles localization at the active zone could contribute to normalize neurotransmission and enhance memory. However, it is possible that mGluR5-PAMs could activate several other neuroplastic mechanisms to enhance memory. Corroborating this hypothesis, in this study, we demonstrated that BACHD treatment with the mGluR5 PAM VU0409551 increased mGluR5 expression at the plasma membrane and triggered the activation of cell signaling pathways important for synaptic plasticity, enhancing the level of dendritic spine maturation and rescuing BACHD memory impairment.

In most cases, receptor activation by an agonist leads to receptor endocytosis and consequent desensitization, avoiding chronic over-stimulation (Hanyaloglu and von Zastrow 2008). However, our results demonstrated that VU0409551 stabilized mGluR5 at the cellular plasma membrane in both the striatum and hippocampus of BACHD mice, but not of WT mice. We hypothesize that this increase in mGluR5 cell surface expression is because of reduced receptor internalization, which has been shown to be regulated by a wide variety of proteins, including G protein-coupled receptor kinase 2 (Ribeiro *et al.* 2009), Ca^{2+}/calmodulin-dependent protein kinase IIα (CaMKIIα) (Raka *et al.* 2015), protein kinase C and calmodulin protein (CaM) (Lee *et al.* 2008). It has been shown that binding of CaM to mGluR5 stabilizes the receptor at the cell membrane (Lee *et al.* 2008). Interestingly, in addition to binding to mGluR5, CaM also interacts directly with wild-type and mutant HTT, binding with higher affinity to mutant HTT (Bao *et al.* 1996). Moreover, it has been shown that mGluR5 also binds to HTT protein (Anborgh *et al.* 2005). CaM is activated by Ca^{2+}, and Ca^{2+} mobilization via mGluR5 increases CaM binding to this receptor (Ko *et al.* 2012). It has been shown that VU0409551, in the presence of glutamate, increases intracellular Ca^{2+} concentration via mGluR5 in a NMDAR-independent mechanism (Rook *et al.* 2015). Thus, we propose that VU0409551 increases CaM activity and that CaM binding to mGluR5 may be enhanced because of the presence of mutated HTT, resulting in increased mGluR5 expression at the cell surface of BACHD mice.

Increased mGluR5 cell surface expression can facilitate the activation of cellular pathways dependent on this receptor and our results demonstrate that VU0409551 treatment of BACHD mice increased the expression of several genes important for synaptic plasticity. Moreover, mGluR5 stimulation modulates the activation of ERK1/2, CaMK, adenylate cyclase, protein kinase C, influencing gene expression through several transcription factors (Yang *et al.* 2004; Hou *et al.* 2006; Ribeiro *et al.* 2010). Among the transcription factors that are regulated by mGluR5, CREB deserves special attention, as it is also regulated by HTT (Li and Li 2004). For instance, mutant HTT aggregates can sequester CREB-binding protein, which is an important activator of CREB, decreasing the expression of CREB target genes (Nucifora *et al.* 2001). Interestingly, reduced expression of CREB targets, including Arc/Arg3.1 and c-Fos, has been associated with memory deficits observed in a HD mouse model, Hdh (Q7/Q111) (Giralt *et al.* 2012). Our results clearly demonstrated that VU0409551 treatment of BACHD mice promoted an increase in the mRNA levels of several genes important for synaptic plasticity, including BDNF, Arc/Arg3.1, and c-Fos. The crucial role of BDNF, c-Fos, and Arc/Arg3.1 on LTP, as well as in spatial and recognition memory has been demonstrated in several studies (Guzowski *et al.* 2000; Mizuno *et al.* 2000; Guzowski 2002; Fleischmann *et al.* 2003; Labrousse *et al.* 2009; Albasser *et al.* 2010). Thus, increased expression of these genes important for synaptic plasticity by VU0409551 treatment could be underlying the memory enhancement observed in BACHD mice. Moreover, increased syntaxin 1A and PSD-95 expression could also contribute to VU0409551-dependent enhancement in memory. Syntaxin 1A is part of the SNARE complex, which is formed by a set of proteins that mediate fusion and exocytosis of vesicles in the pre-synaptic terminal (Bennett *et al.* 1992). It has been demonstrated that mutated HTT protein alters pre-synaptic vesicle release and neurotransmission (Trushina *et al.* 2004; Milnerwood and Raymond 2007). Thus, syntaxin 1A increased expression in BACHD mice

could contribute to normalize HD-mediated neurotransmission alterations. Interestingly, syntaxin 1A expression was increased in both the hippocampus and striatum of BACHD mice following VU0409551 treatment, although the other tested genes that are also regulated by CREB, including c-Fos, BDNF, Arc/Arg3.1, were increased only in the hippocampus, but not in the striatum. Therefore, it is possible that region specific factors could be altering the induction of expression by CREB or even that other transcription regulators that are differentially expressed in the striatum and hippocampus could be influencing the expression of these genes. Future studies will be important to investigate this hypothesis.

Increased levels of c-Fos, Arc/Arg3.1, syntaxin 1A, and PSD-95 also contribute to an increase in the number of pre- and post-synaptic terminals, enhancing dendritic spine density and maturation, which is crucial for memory consolidation (El-Husseini *et al.* 2000; Plath *et al.* 2006; Shepherd *et al.* 2006; Edling *et al.* 2007; Guo *et al.* 2010). It is well known that more than 90% of the excitatory axodendritic synapses in the cortex occur on dendritic spines (Hering and Sheng 2001). Throughout development, dendritic spines undergo changes in their morphology in a mechanism that is directly related to their function. For example, the immature spine shapes (filopodia, long, and thin) are highly motile and can initiate synaptic contact (Ziv and Smith 1996). Mature spine shapes (stubby, mushroom, and branched) are more stable and contain an abundance of receptors that maintain high levels of synaptic activity (Chang and Greenough 1984; Harris *et al.* 1992; Hering and Sheng 2001). Reduction in dendritic spine density has been reported in HD patients (Graveland *et al.* 1985), as well as in BACHD mice (Simmons *et al.* 2013). Our analyses showed that BACHD mice exhibited decreased number of dendritic spines, as compared to that of WT, and that VU0409551 treatment rescued this phenotype. Notably, VU0409551 treatment increased the number of mushroom-like spines in both WT and BACHD mice and enhanced the number of branched spines in WT mice. These results are in agreement with previously published data demonstrating that CDPPB subchronic treatment increased density and number of mushroom spines in rats trained to self-administer alcohol (Gass *et al.* 2014). Moreover, our results indicate that the increase in post-synaptic sites triggered by VU0409551 treatment was followed by enhanced number of pre-synaptic terminals in BACHD mice. Thus, our data demonstrating that VU0409551 treatment for only 8 days suffice to increase spine maturation and pre-synaptic terminal density in a mouse model of HD clearly represents a relevant mechanism that could be underlying VU0409551-dependent memory enhancement. Together, these data suggest that VU0409551 is a drug with therapeutic potential to reverse memory impairment, a common finding of a number of neurodegenerative diseases.

Supplementary Material

Refer to Web version on PubMed Central for supplementary material.

Acknowledgments

Acknowledgments and conflict of interest disclosure

We thank Dr Gustavo B. Menezes for providing the equipment and technical support for confocal microscopy experiments. This work was supported by CNPq (grant number 400133/2014-8) and FAPEMIG (grant number APQ-00294-15) grants to F. M. R. The authors have no conflict of interest to declare.

All experiments were conducted in compliance with the ARRIVE guidelines.

Abbreviations used:

AKT	protein kinase B
Arc/Arg3.1	cytoskeletal-associated protein
BDNF	brain-derived neurotrophic factor
BSA	bovine serum albumin
CaM	calmodulin protein
CaMKIIα	Ca^{2+}/calmodulin-dependent protein kinase IIα
CBP	CREB-binding protein
CDPPB	3- Cyano-N-(1,3-diphenyl-1H-pyrazol-5-yl)benzamide
CREB	cAMP-responsive element
CS	conditioning stimulus
DIV	days *in vitro*
DMSO	dimethyl sulfoxide
ERK	extracellular signal-regulated kinase
GRK2	G protein-coupled receptor kinase 2
HBSS	Hank’s balanced salt solution
HD	Huntington’s disease
HTT	huntingtin
i.p.	intraperitoneal injection
InsP3	inositol-1,4,5-triphosphate
LTD	long-term depression
LTP	long-term potentiation
mGluR	metabotropic glutamate receptor
NMDAR	N-methyl-D-aspartate receptor
PAM	positive allosteric modulator
PBS	phosphate-buffered saline

PKC	protein kinase C
PSD-95	post-synaptic density-95
RT-qPCR	quantitative reverse transcriptase polymerase chain reaction
VU0409551	[6,7-Dihydro-2-(phenoxymethyl)oxazolo [5,4-*c*]pyridin-5(4*H*)-yl](fluorophenyl)methanone
WT	wild type

References

Agerman K, Hjerling-Leffler J, Blanchard MP, Scarfone E, Canlon B, Nosrat C and Ernfors P (2003) BDNF gene replacement reveals multiple mechanisms for establishing neurotrophin specificity during sensory nervous system development. Development 130, 1479–1491. [PubMed: 12620975]

Albasser MM, Poirier GL and Aggleton JP (2010) Qualitatively different modes of perirhinal-hippocampal engagement when rats explore novel vs. familiar objects as revealed by c-Fos imaging. Eur. J. Neuorsci 31, 134–147.

Anborgh PH, Godin C, Pampillo M, Dhami GK, Dale LB, Cregan SP, Truant R and Ferguson SS (2005) Inhibition of metabotropic glutamate receptor signaling by the huntingtin-binding protein optineurin. J. Biol. Chem 280, 34840–34848. [PubMed: 16091361]

Ayala JE, Chen Y, Banko JL, et al. (2009) mGluR5 positive allosteric modulators facilitate both hippocampal LTP and LTD and enhance spatial learning. Neuropsychopharmacology 34, 2057–2071. [PubMed: 19295507]

Baake V, Reijntjes R, Dumas EM, Thompson JC and Network R. I. o. t. E. H. s. D. and Roos RAC (2017) Cognitive decline in Huntington's disease expansion gene carriers. Cortex, 95, 51–62. [PubMed: 28843844]

Bailey KR and Crawley JN (2009) Anxiety-related behaviors in mice, in Methods of Behavior Analysis in Neuroscience (Buccafusco JJ ed.), Chapter 5, pp. 1–24. Boca Raton, FL, CRC Press/Taylor & Francis.

Bao J, Sharp AH, Wagster MV, Becher M, Schilling G, Ross CA, Dawson VL and Dawson TM (1996) Expansion of polyglutamine repeat in huntingtin leads to abnormal protein interactions involving calmodulin. Proc. Natl Acad. Sci. USA 93, 5037–5042. [PubMed: 8643525]

Batista EM, Doria JG, Ferreira-Vieira TH, Alves-Silva J, Ferguson SS, Moreira FA and Ribeiro FM (2016) Orchestrated activation of mGluR5 and CB1 promotes neuroprotection. Mol. Brain 9, 80. [PubMed: 27543109]

Bennett MK, Calakos N and Scheller RH (1992) Syntaxin: a synaptic protein implicated in docking of synaptic vesicles at presynaptic active zones. Science 257, 255–259. [PubMed: 1321498]

Caine ED, Hunt RD, Weingartner H and Ebert MH (1978) Huntington's dementia. Clinical and neuropsychological features. Arch. Gen. Psychiatry 35, 377–384. [PubMed: 153122]

Chang FL and Greenough WT (1984) Transient and enduring morphological correlates of synaptic activity and efficacy change in the rat hippocampal slice. Brain Res. 309, 35–46. [PubMed: 6488013]

Doria JG, Silva FR, de Souza JM, Vieira LB, Carvalho TG, Reis HJ, Pereira GS, Dobransky T and Ribeiro FM (2013) Metabotropic glutamate receptor 5 positive allosteric modulators are neuroprotective in a mouse model of Huntington's disease. Br. J. Pharmacol 169, 909–921. [PubMed: 23489026]

Doria JG, de Souza JM, Andrade JN, Rodrigues HA, Guimaraes IM, Carvalho TG, Guatimosim C, Dobransky T and Ribeiro FM (2015) The mGluR5 positive allosteric modulator, CDPPB, ameliorates pathology and phenotypic signs of a mouse model of Huntington's disease. Neurobiol. Dis 73, 163–173. [PubMed: 25160573]

Edling Y, Ingelman-Sundberg M and Simi A (2007) Glutamate activates c-fos in glial cells via a novel mechanism involving the glutamate receptor subtype mGlu5 and the transcriptional repressor DREAM. Glia 55, 328–340. [PubMed: 17120244]

El-Husseini AE, Schnell E, Chetkovich DM, Nicoll RA and Bredt DS (2000) PSD-95 involvement in maturation of excitatory synapses. Science 290, 1364–1368. [PubMed: 11082065]

Fan J, Cowan CM, Zhang LY, Hayden MR and Raymond LA (2009) Interaction of postsynaptic density protein-95 with NMDA receptors influences excitotoxicity in the yeast artificial chromosome mouse model of Huntington's disease. J. Neurosci 29, 10928–10938. [PubMed: 19726651]

Ferreira LT, Dale LB, Ribeiro FM, Babwah AV, Pampillo M and Ferguson SS (2009) Calcineurin inhibitor protein (CAIN) attenuates Group I metabotropic glutamate receptor endocytosis and signaling. J. Biol. Chem 284, 28986–28994. [PubMed: 19717561]

Fleischmann A, Hvalby O, Jensen V, et al. (2003) Impaired long-term memory and NR2A-type NMDA receptor-dependent synaptic plasticity in mice lacking c-Fos in the CNS. J. Neurosci 23, 9116–9122. [PubMed: 14534245]

Gass JT, Trantham-Davidson H, Kassab AS, Glen WB, Jr, Olive MF and Chandler LJ (2014) Enhancement of extinction learning attenuates ethanol-seeking behavior and alters plasticity in the prefrontal cortex. J. Neurosci 34, 7562–7574. [PubMed: 24872560]

Giralt A, Puigdellivol M, Carreton O, Paoletti P, Valero J, Parra-Damas A, Saura CA, Alberch J and Gines S (2012) Long-term memory deficits in Huntington's disease are associated with reduced CBP histone acetylase activity. Hum. Mol. Genet 21, 1203–1216. [PubMed: 22116937]

Graveland GA, Williams RS and DiFiglia M (1985) Evidence for degenerative and regenerative changes in neostriatal spiny neurons in Huntington's disease. Science 227, 770–773. [PubMed: 3155875]

Gray M, Shirasaki DI, Cepeda C, et al. (2008) Full-length human mutant huntingtin with a stable polyglutamine repeat can elicit progressive and selective neuropathogenesis in BACHD mice. J. Neurosci 28, 6182–6195. [PubMed: 18550760]

Group, T. H. s. D. C. R (1993) A novel gene containing a trinucleotide repeat that is expanded and unstable on Huntington's disease chromosomes. Cell 72, 971–983. [PubMed: 8458085]

Guo CH, Senzel A, Li K and Feng ZP (2010) De novo protein synthesis of syntaxin-1 and dynamin-1 in long-term memory formation requires CREB1 gene transcription in Lymnaea stagnalis. Behav. Genet 40, 680–693. [PubMed: 20563839]

Guzowski JF (2002) Insights into immediate-early gene function in hippocampal memory consolidation using antisense oligonucleotide and fluorescent imaging approaches. Hippocampus 12, 86–104. [PubMed: 11918292]

Guzowski JF, Lyford GL, Stevenson GD, Houston FP, McGaugh JL, Worley PF and Barnes CA (2000) Inhibition of activity-dependent arc protein expression in the rat hippocampus impairs the maintenance of long-term potentiation and the consolidation of long-term memory. J. Neurosci 20, 3993–4001. [PubMed: 10818134]

Hanyaloglu AC and von Zastrow M (2008) Regulation of GPCRs by endocytic membrane trafficking and its potential implications. Annu. Rev. Pharmacol. Toxicol 48, 537–568. [PubMed: 18184106]

Harris KM, Jensen FE and Tsao B (1992) Three-dimensional structure of dendritic spines and synapses in rat hippocampus (CA1) at postnatal day 15 and adult ages: implications for the maturation of synaptic physiology and long-term potentiation. J. Neurosci. 12, 2685–2705. [PubMed: 1613552]

Hering H and Sheng M (2001) Dendritic spines: structure, dynamics and regulation. Nat. Rev. Neurosci 2, 880–888. [PubMed: 11733795]

Hodges JR, Salmon DP and Butters N (1992) Semantic memory impairment in Alzheimer's disease: failure of access or degraded knowledge? Neuropsychologia 30, 301–314. [PubMed: 1603295]

Hou L, Antion MD, Hu D, Spencer CM, Paylor R and Klann E (2006) Dynamic translational and proteasomal regulation of fragile X mental retardation protein controls mGluR-dependent long-term depression. Neuron 51, 441–454. [PubMed: 16908410]

Ko SJ, Isozaki K, Kim I, et al. (2012) PKC phosphorylation regulates mGluR5 trafficking by enhancing binding of Siah-1A. J. Neurosci 32, 16391–16401. [PubMed: 23152621]

Labrousse VF, Costes L, Aubert A, Darnaudery M, Ferreira G, Amedee T and Laye S (2009) Impaired interleukin-1beta and c-Fos expression in the hippocampus is associated with a spatial memory deficit in P2X(7) receptor-deficient mice. PLoS ONE 4, e6006. [PubMed: 19547756]

Lazaroni TL, Raslan AC, Fontes WR, de Oliveira ML, Bader M, Alenina N, Moraes MF, Dos Santos RA and Pereira GS (2012) Angiotensin-(1-7)/Mas axis integrity is required for the expression of object recognition memory. Neurobiol. Learn. Mem 97, 113–123. [PubMed: 22067210]

Lee JH, Lee J, Choi KY, et al. (2008) Calmodulin dynamically regulates the trafficking of the metabotropic glutamate receptor mGluR5. Proc. Natl Acad. Sci. USA 105, 12575–12580. [PubMed: 18715999]

Li SH and Li XJ (2004) Huntingtin-protein interactions and the pathogenesis of Huntington's disease. Trends in genetics : TIG 20, 146–154. [PubMed: 15036808]

Milnerwood AJ and Raymond LA (2007) Corticostriatal synaptic function in mouse models of Huntington's disease: early effects of huntingtin repeat length and protein load. J. Physiol 585, 817–831. [PubMed: 17947312]

Mizuno M, Yamada K, Olariu A, Nawa H and Nabeshima T (2000) Involvement of brain-derived neurotrophic factor in spatial memory formation and maintenance in a radial arm maze test in rats. J. Neurosci 20, 7116–7121. [PubMed: 10995859]

Nimchinsky EA, Sabatini BL and Svoboda K (2002) Structure and function of dendritic spines. Annu. Rev. Physiol 64, 313–353. [PubMed: 11826272]

Nucifora FC, Jr, Sasaki M, Peters MF, et al. (2001) Interference by huntingtin and atrophin-1 with cbp-mediated transcription leading to cellular toxicity. Science 291, 2423–2428. [PubMed: 11264541]

Plath N, Ohana O, Dammermann B, et al. (2006) Arc/Arg3.1 is essential for the consolidation of synaptic plasticity and memories. Neuron 52, 437–444. [PubMed: 17088210]

Radwanska K, Medvedev NI, Pereira GS, et al. (2011) Mechanism for long-term memory formation when synaptic strengthening is impaired. Proc. Natl Acad. Sci. USA 108, 18471–18475. [PubMed: 22025701]

Raka F, Di Sebastiano AR, Kulhawy SC, Ribeiro FM, Godin CM, Caetano FA, Angers S and Ferguson SS (2015) Ca(2 +)/calmodulin-dependent protein kinase II interacts with group I metabotropic glutamate and facilitates receptor endocytosis and ERK1/2 signaling: role of beta-amyloid. Mol. Brain 8, 21. [PubMed: 25885040]

Reichel CM, Schwendt M, McGinty JF, Olive MF and See RE (2011) Loss of object recognition memory produced by extended access to methamphetamine self-administration is reversed by positive allosteric modulation of metabotropic glutamate receptor 5. Neuropsychopharmacology 36, 782–792. [PubMed: 21150906]

Ribeiro FM, Ferreira LT, Paquet M, Cregan T, Ding Q, Gros R and Ferguson SS (2009) Phosphorylation-independent regulation of metabotropic glutamate receptor 5 desensitization and internalization by G protein-coupled receptor kinase 2 in neurons. J. Biol. Chem 284, 23444–23453. [PubMed: 19564331]

Ribeiro FM, Paquet M, Cregan SP and Ferguson SS (2010) Group I metabotropic glutamate receptor signalling and its implication in neurological disease. S Neurol Disord Drug Targets 9, 574–595.

Risher WC, Ustunkaya T, Singh Alvarado J and Eroglu C (2014) Rapid Golgi analysis method for efficient and unbiased classification of dendritic spines. PLoS ONE 9, e107591. [PubMed: 25208214]

Rook JM, Xiang Z, Lv X, et al. (2015) Biased mGlu5-Positive Allosteric Modulators Provide In Vivo Efficacy without Potentiating mGlu5 Modulation of NMDAR Currents. Neuron 86, 1029–1040. [PubMed: 25937172]

Saykin AJ, Gur RC, Gur RE, Mozley PD, Mozley LH, Resnick SM, Kester DB and Stafiniak P (1991) Neuropsychological function in schizophrenia. Selective impairment in memory and learning. Arch. Gen. Psychiatry 48, 618–624. [PubMed: 2069492]

Shepherd JD, Rumbaugh G, Wu J, Chowdhury S, Plath N, Kuhl D, Huganir RL and Worley PF (2006) Arc/Arg3.1 mediates homeostatic synaptic scaling of AMPA receptors. Neuron 52, 475–484. [PubMed: 17088213]

Silva FR, Miranda AS, Santos RPM, Olmo IG, Zamponi GW, Dobransky T, Cruz JS, Vieira LB and Ribeiro FM (2017) N-type Ca2 + channels are affected by full-length mutant huntingtin expression in a mouse model of Huntington's disease. Neurobiol. Aging 55, 1–10. [PubMed: 28391067]

Simmons DA, Belichenko NP, Yang T, Condon C, Monbureau M, Shamloo M, Jing D, Massa SM and Longo FM (2013) A small molecule TrkB ligand reduces motor impairment and neuropathology in R6/2 and BACHD mouse models of Huntington's disease. J. Neurosci 33, 18712–18727. [PubMed: 24285878]

Simonyi A, Schachtman TR and Christoffersen GR (2010) Metabotropic glutamate receptor subtype 5 antagonism in learning and memory. Eur. J. Pharmacol 639, 17–25. [PubMed: 20363219]

Trushina E, Dyer RB, Badger JD, 2nd, et al. (2004) Mutant huntingtin impairs axonal trafficking in mammalian neurons in vivo and in vitro. Mol. Cell. Biol 24, 8195–8209. [PubMed: 15340079]

Tyler WJ and Pozzo-Miller L (2003) Miniature synaptic transmission and BDNF modulate dendritic spine growth and form in rat CA1 neurones. J. Physiol 553, 497–509. [PubMed: 14500767]

Uslaner JM, Parmentier-Batteur S, Flick RB, Surles NO, Lam JS, McNaughton CH, Jacobson MA and Hutson PH (2009) Dose-dependent effect of CDPPB, the mGluR5 positive allosteric modulator, on recognition memory is associated with GluR1 and CREB phosphorylation in the prefrontal cortex and hippocampus. Neuropharmacology 57, 531–538. [PubMed: 19627999]

Vonsattel JP (2008) Huntington disease models and human neuropathology: similarities and differences. Acta Neuropathol. 115, 55–69. [PubMed: 17978822]

Vonsattel JP, Myers RH, Stevens TJ, Ferrante RJ, Bird ED and Richardson EP, Jr (1985) Neuropathological classification of Huntington's disease. J. Neuropathol. Exp. Neurol 44, 559–577. [PubMed: 2932539]

Xing J, Ginty DD and Greenberg ME (1996) Coupling of the RAS-MAPK pathway to gene activation by RSK2, a growth factor-regulated CREB kinase. Science 273, 959–963. [PubMed: 8688081]

Yang L, Mao L, Tang Q, Samdani S, Liu Z and Wang JQ (2004) A novel Ca2 + -independent signaling pathway to extracellular signal-regulated protein kinase by coactivation of NMDA receptors and metabotropic glutamate receptor 5 in neurons. J. Neurosci 24, 10846–10857. [PubMed: 15574735]

Yin Y, Edelman GM and Vanderklish PW (2002) The brain-derived neurotrophic factor enhances synthesis of Arc in synaptoneurosomes. Proc. Natl Acad. Sci. USA 99, 2368–2373. [PubMed: 11842217]

Ziv NE and Smith SJ (1996) Evidence for a role of dendritic filopodia in synaptogenesis and spine formation. Neuron 17, 91–102. [PubMed: 8755481]

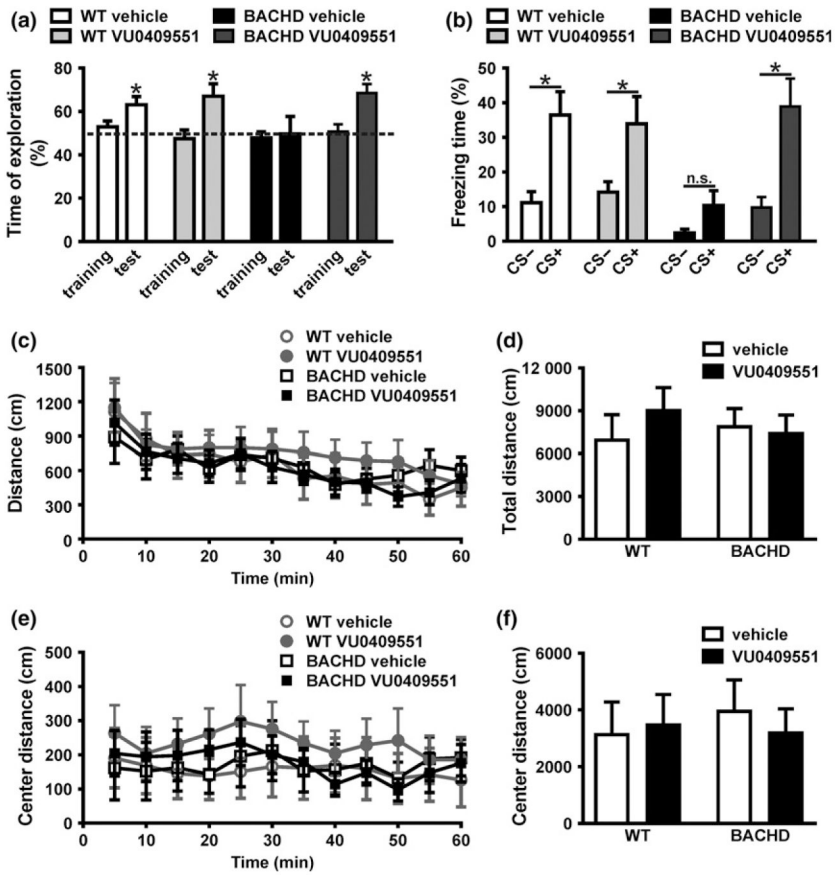

Fig. 1.

VU0409551 treatment improved BACHD memory without altering locomotion. (a) Graph shows time of object exploration by wild-type (WT) and BACHD mice, calculated as the recognition index for the training and test phases. A score of 50% indicates no preference. Data represent the means ± SEM, $n = 7–9$. * indicates significant difference from chance exploration (50%) ($p < 0.05$). (b) Graph shows the freezing response of WT and BACHD mice in the presence (+) or absence (−) of conditioning stimulus (CS). Data represent the means ± SEM, expressed as percentage of freezing time during CS+ and CS−, $n = 7–9$. * indicates significant difference comparing CS+ and CS− ($p < 0.05$) and 'n.s.' indicates no difference comparing CS+ and CS−. Graphs show the distance travelled by WT and BACHD mice every 5 min (c), as well as the total distance travelled over 60 min (d) in the open field apparatus. Graphs also show the distance travelled by WT and BACHD mice every 5 min (e), as well as the total distance travelled over 60 min (f) in the center of the open field apparatus. Data represent the means ± SEM. Number of mice: WT-vehicle $n = 7$, WT-VU0409551 $n = 8$, BACHD-vehicle $n = 8$, and BACHD-VU0409551 $n = 9$.

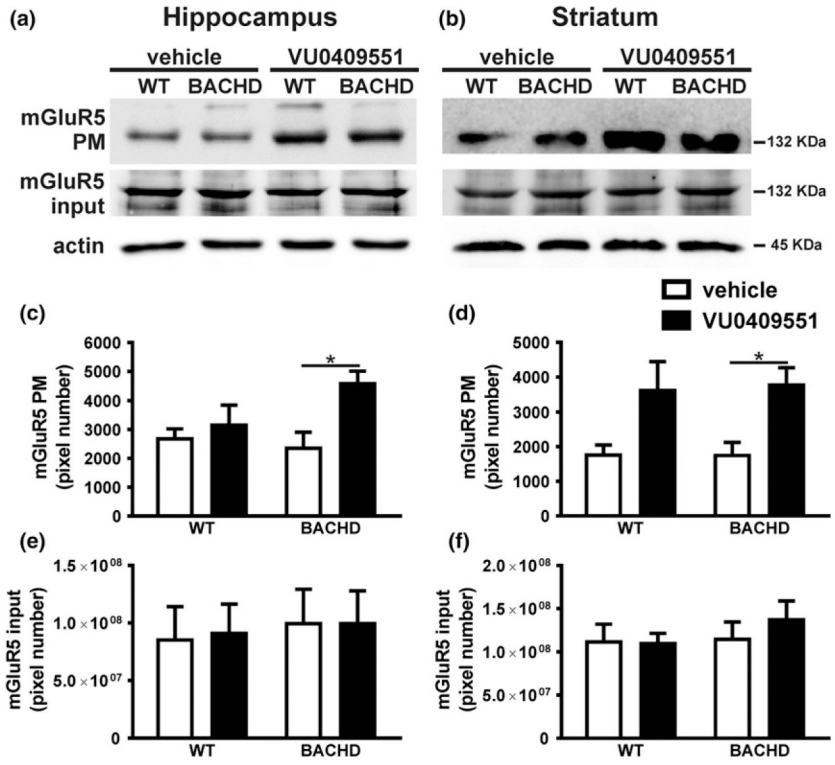

Fig. 2.

VU0409551 treatment increased mGluR5 cell surface expression in BACHD mice. Shown are representative immunoblots for mGluR5 cell surface (upper panel) and total cell lysate expression (middle panel), as well as representative immunoblots for actin (lower panel) in hippocampal (a) and striatal (b) slices of wild-type (WT) and BACHD mice, treated with either vehicle or VU0409551. Graphs show the densitometric analysis of the cell surface expression of mGluR5 in hippocampal (c) and striatal (d) slices, as well as mGluR5 total cell lysate expression in hippocampal (e) and striatal (f) slices of WT and BACHD mice, treated with either vehicle or VU0409551. Data represent the mean ± SEM. Number of mice: $n = 4$. ♦indicates significant difference ($p < 0.05$).

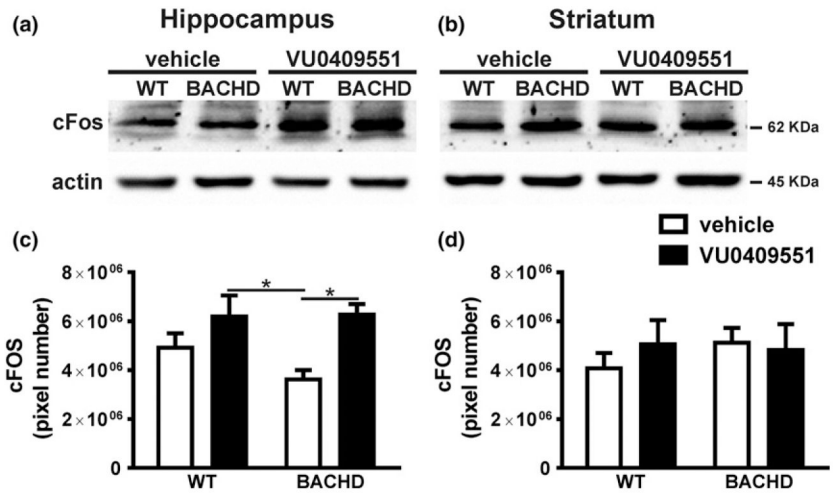

Fig. 3.

VU0409551 treatment enhanced c-Fos expression in BACHD mice. Shown are representative immunoblots for c-Fos (upper panel) and actin (lower panel) expression in the hippocampus (a) and striatum (b) of wild-type (WT) and BACHD mice, treated with either vehicle or VU0409551. 80 μg of total cell lysate was used for each sample. Graphs show the densitometric analysis of c-Fos expression in the hippocampus (a) and striatum (b) of WT and BACHD mice, treated with either vehicle or VU0409551. Data represent the means ± SEM. Number of mice: WT-vehicle $n = 6$, WT-VU0409551 $n = 5$, BACHD-vehicle $n = 6$, and BACHD-VU0409551 $n = 5$. *indicates significant difference ($p < 0.05$).

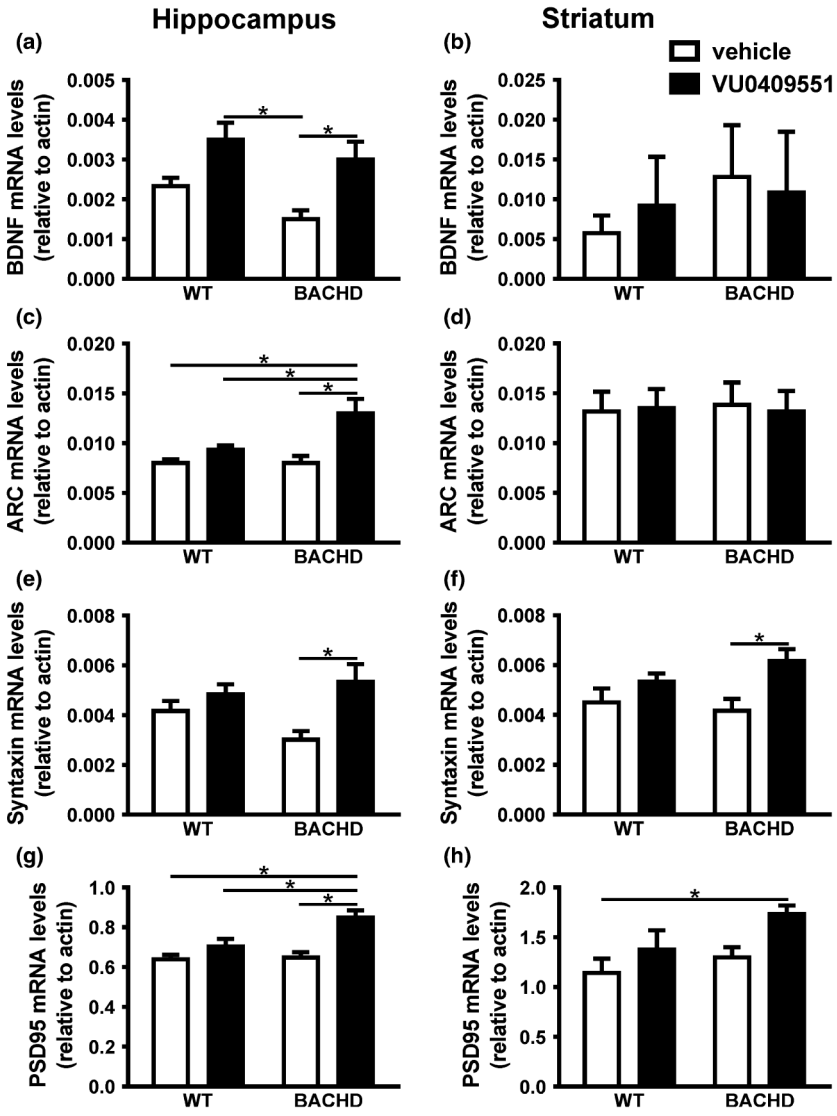

Fig. 4.

VU0409551 treatment increased the expression of genes important for synaptic plasticity. Graphs show brain-derived neurotrophic factor (BDNF) mRNA levels in the hippocampus (a) and striatum (b), Arc/Arg3.1 mRNA levels in the hippocampus (c) and striatum (d), syntaxin 1A mRNA levels in the hippocampus (e) and striatum (f) and post-synaptic density-95 (PSD-95) mRNA levels in the hippocampus (g) and striatum (h) of wild-type (WT) and BACHD mice, treated with either vehicle or VU0409551. mRNA levels were assessed by RT-qPCR, which was performed in triplicate and normalized to actin mRNA levels. Data represent the means ± SEM. Number of mice: $n = 6$. indicates significant difference ($p < 0.05$).

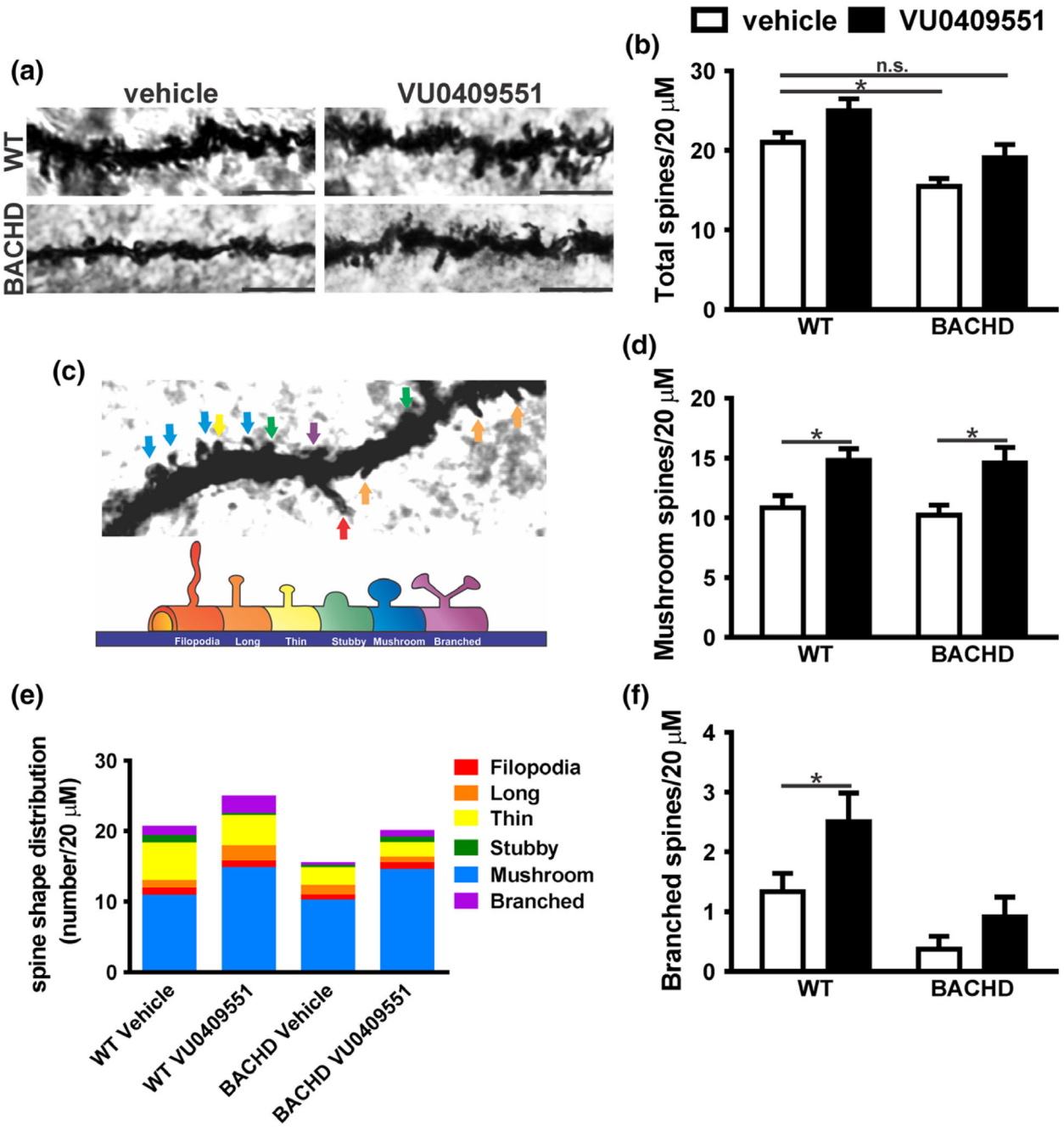

Fig. 5.

VU0409551 treatment increased dendritic spine maturation. (a) Shown are representative confocal micrographs from tertiary dendrites of hippocampal neurons from wild-type (WT) and BACHD mice, treated with either vehicle or VU0409551. Dendrite segments shown are 20 μm in length and size bar corresponds to 5 μm. (b) Graph shows dendritic spine density (total number of dendritic spines per 20 μm). (c) Upper image: Confocal image of a dendrite containing all possible shapes of dendritic spines, which are pointed by colored arrows. Lower image: Schematic drawing of spines shown in: red: filopodia; orange: long; yellow: thin; green: stubby; blue: mushroom; purple: branched. (e) Colored graph shows the

contribution of each type of spine per 20 μm of dendrite segment. Graphs show the total number of mature mushroom (d) and branched (f) spines per 20 μm of dendrite segment. Data represent the mean ± SEM. Number of dendrites: WT-vehicle $n = 15$, WT-VU0409551 $n = 12$, BACHD-vehicle $n = 12$, and BACHD-VU0409551 $n = 12$. *Indicates significant difference ($p < 0.05$).

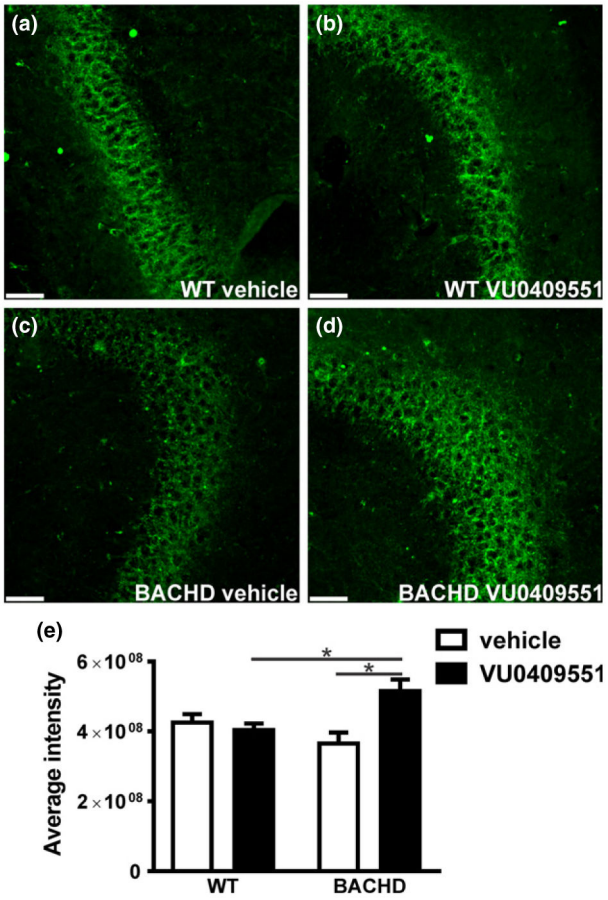

Fig. 6.

VU0409551 treatment enhanced the number of presynaptic terminals. Shown are laser-scanning confocal micrographs from hippocampal slices obtained from wild-type (WT) mice, treated with either vehicle (a) or VU0409551 (b), and BACHD mice, treated with either vehicle (c) or VU0409551 (d), and immunolabeled for synaptotagmin 2 (green). Scale bar = 50 μM. (e) Graph shows average intensity of pixel gray levels of synaptotagmin 2. Data represent the mean ± SEM. Number of images: $n = 18$. *Indicates significant difference ($p < 0.05$).